



HAL
open science

The magnetic signal from trunk bark of urban trees catches the variation in particulate matter exposure within and across six European cities

Anskje van Mensel, Karen Wuyts, Pedro Pinho, Babette Muyshondt, Cristiana Aleixo, Marta Alos Orti, Joan Casanelles-Abella, François Chiron, Tiit Hallikma, Lauri Laanisto, et al.

► To cite this version:

Anskje van Mensel, Karen Wuyts, Pedro Pinho, Babette Muyshondt, Cristiana Aleixo, et al.. The magnetic signal from trunk bark of urban trees catches the variation in particulate matter exposure within and across six European cities. *Environmental Science and Pollution Research*, In press, 10.1007/s11356-023-25397-8 . hal-04002043

HAL Id: hal-04002043

<https://hal.science/hal-04002043>

Submitted on 23 Feb 2023

HAL is a multi-disciplinary open access archive for the deposit and dissemination of scientific research documents, whether they are published or not. The documents may come from teaching and research institutions in France or abroad, or from public or private research centers.

L'archive ouverte pluridisciplinaire **HAL**, est destinée au dépôt et à la diffusion de documents scientifiques de niveau recherche, publiés ou non, émanant des établissements d'enseignement et de recherche français ou étrangers, des laboratoires publics ou privés.

1 **The magnetic signal from trunk bark of urban trees catches the variation in particulate matter**
2 **exposure within and across six European cities**

3 Anskje VAN MENDEL^{a,*}, Karen WUYTS^a, Pedro PINHO^b, Babette MUYSHONDT^a, Cristiana ALEIXO^b, Marta
4 ALOS ORTI^c, Joan CASANELLES-ABELLA^{d,e}, François CHIRON^f, Tiit HALLIKMA^c, Lauri LAANISTO^c, Marco
5 MORETTI^d, Ülo NIINEMETS^g, Piotr TRYJANOWSKI^h, Roeland SAMSON^a

6
7 ^a Laboratory of Environmental and Urban Ecology, Department of Bioscience Engineering, University
8 of Antwerp, Antwerp, Belgium

9 ^b Centre for Ecology, Evolution and Environmental Changes (CE3c), Faculdade de Ciências da
10 Universidade de Lisboa, Lisbon, Portugal

11 ^c Chair of Biodiversity and Nature Tourism, Estonian University of Life Sciences, Tartu, Estonia

12 ^d Biodiversity and Conservation Biology, Swiss Federal Research Institute WSL, Birmensdorf,
13 Switzerland

14 ^e Landscape Ecology, Institute of Terrestrial Ecosystems, ETH Zurich, Zurich, Switzerland

15 ^f Université Paris-Saclay, CNRS, AgroParisTech, Ecologie Systématique Evolution, 91405, Orsay, France

16 ^g Chair of Crop Science and Plant Biology, Estonian University of Life Sciences, Tartu, Estonia

17 ^h Department of Zoology, Poznan University of Life Sciences, Poland

18

19 * Corresponding author: Anskje VAN MENDEL; email address: anskje.vanmensele@uantwerpen.be;
20 telephone number: +32 (0) 3 265 96 04

21

22 **Abstract**

23 Biomagnetic monitoring increasingly is applied to assess particulate matter (PM) concentrations,
24 mainly using plant leaves sampled in small geographical area and from a limited number of species.
25 Here, the potential of magnetic analysis of urban tree trunk bark to discriminate between PM exposure
26 levels was evaluated and bark magnetic variation was investigated at different spatial scales. Trunk
27 bark was sampled from 684 urban trees of 39 genera in 173 urban green areas across six European
28 cities. Samples were analysed magnetically for the Saturation Isothermal Remanent Magnetisation
29 (SIRM). The bark SIRM reflected well the PM exposure level at city and local scale, as the bark SIRM (i)
30 differed between the cities in accordance with the mean atmospheric PM concentrations and (ii)
31 increased with the cover of roads and industrial area around the trees. Furthermore, with increasing
32 tree circumferences, the SIRM values increased, as a reflection of a tree age effect related to PM
33 accumulation over time. Moreover, bark SIRM was higher at the side of the trunk facing the prevailing
34 wind direction. Significant relationships between SIRM of different genera validate the possibility to

35 combine bark SIRM from different genera to improve sampling resolution and coverage in biomagnetic
36 studies. Thus, the SIRM signal of trunk bark from urban trees is a reliable proxy for atmospheric coarse
37 to fine PM exposure in areas dominated by one PM source, as long as variation caused by genus,
38 circumference and trunk side is taken into account.

39

40 **Keywords**

41 Magnetic biomonitoring – urban green - tree trunk bark - SIRM – air pollution – particulate matter

42

43 **Acknowledgements**

44 This study was supported by the Belgian Science Policy (Belspo) within the Belgian research action
45 through interdisciplinary networks (BRAIN-be) with project number BR/175/A1/BIOVEINS-BE. This was
46 within the framework of the ERA-NET BiodivERsA project ‘BIOVEINS - Connectivity of green and blue
47 infrastructures: living veins for biodiverse and healthy cities’ (H2020 BiodivERsA32015104). A. Van
48 Mensel, R. Samson and K. Wuyts acknowledge funding from the University of Antwerp. P. Pinho
49 acknowledges Fundação para a Ciência e a Tecnologia (FCT, 2020.03415.CEECIND). B. Muyshondt
50 acknowledges funding from a PhD grant Strategic Basic Research of the Research Foundation - Flanders
51 (FWO, 1S84819N). C. Aleixo gratefully acknowledges FCT for the financial support (PhD grant reference
52 SFRH/BD/141822/2018). M. Alos Orti was supported by the European Social Fund’s Dora Plus
53 Programme. J. Casanelles-Abella was supported by the Swiss National Science Foundation (project
54 31BD30_172467). P. Tryjanowski acknowledges the National Science Center Poland (NCN) for funding
55 through NCN/2016/22/Z/NZ8/00004. Moreover, we are grateful to Leen Van Ham and Hanne
56 Hendrickx for laboratory assistance and to Joana Marques and Piret Lõhmus for help with sample
57 collection.

58 **1. Introduction**

59 Air pollution is responsible for millions of premature human deaths worldwide every year (WHO 2018).
60 Particulate matter (PM) – a complex and varying mixture of particles – is one of Europe’s most harmful
61 pollutants for human health (EEA 2020). Suspended in the air, PM can be inhaled and cause various
62 adverse health effects, including aggravation of respiratory and cardiovascular diseases (Pöschl 2005).
63 This is of particular concern in cities since urban air quality is worse than in the rural environment (EEA
64 2020). Air pollution has a direct economic impact, with rising cost for health insurances, reduced labour
65 productivity and higher absenteeism at work (European Environment Agency (EEA) 2020).

66
67 To estimate exposure to air pollution and potential health risks, it is important to monitor local air
68 quality. Especially valuable are easy to measure proxies that integrate the pollution signal over time
69 and provide a reliable estimate of air pollution level in any chosen locality. Biomagnetic monitoring,
70 i.e. the measurement of magnetic variables such as the Saturation Isothermal Remanent
71 Magnetisation (SIRM) of biological matrices exposed to the atmosphere, has been used increasingly
72 over the years to provide proxies of atmospheric PM concentration and of the amount and
73 composition of surface-accumulated PM and metals (Hofman et al. 2017). It is a straightforward, quick
74 method that allows the analysis of a lot of samples to create time-integrated air pollution maps at high
75 spatial resolution while taking into account specific local conditions (as opposed to air quality sampling
76 with sensors or air pollution modelling). Via deposition of PM on exposed surfaces, SIRM is related to
77 atmospheric mass concentrations of coarse and fine PM fractions (PM₁₀ and PM_{2.5}, i.e. PM with an
78 aerodynamic diameter smaller than 10 and 2.5 µm, respectively ; Hofman et al. 2020, Revuelta et al.
79 2014) and increases with exposure to motorised road and railroad traffic (Kardel et al. 2012; Wuyts et
80 al. 2018) and industrial emissions (Matzka and Maher 1999; Declercq et al. 2020). For more
81 background information on SIRM we refer to the review paper by Hofman et al. (2017).

82
83 Mosses, lichens, plant leaves and branches and even animals and human tissues have been used for
84 biomagnetic monitoring (Hofman et al. 2017). So far, the magnetic signal of tree bark from trunk and
85 branches has been only sparsely studied before, although some benefits can be deduced from its use.
86 Trunk bark from *Acer rubrum* trees near a highway was studied by Kletetschka et al. (2003) and showed
87 higher SIRM values at the forest-facing side as opposed to the road-facing side of trees. This difference
88 was presumed to be due to differences in surface wetness. Also Zhang et al. (2008) found that the
89 acquisition of magnetic particles by *Salix matsudana* trunk bark depends on orientation and height.
90 However, they found higher SIRM values at the pollution-source facing sides of trees. Brignole et al.
91 (2018) and Chaparro et al. (2020) showed that magnetic analysis of trunk bark is a good proxy for iron-
92 rich fine particles trapped in the bark and overall load of trace elements in the bark and that it could

93 be used to make a distinction between locations with differences in air pollution. A study on branch
94 bark of *Platanus x acerifolia* (Wuyts et al. 2018) confirmed the presence of metal-containing particles
95 on and in bark and the potential of bark SIRM to distinguish between sites with different traffic
96 intensity, but also pointed to the accumulation of particles and SIRM with exposure time. To develop
97 a reliable methodology for PM exposure assessment based on biomagnetic monitoring with tree bark,
98 potentially confounding factors need to be identified and knowledge on the influence of tree
99 characteristics and sampling methods on the magnetic signal of tree bark is necessary. The available
100 evidence is, however, limited and ambiguous. Moreover, previous studies are predominantly single-
101 city studies which limits the number of species, climate types, PM exposure levels and PM source types,
102 and hence questions the generalizability of the biomagnetic approach.

103

104 In this study, we aimed to evaluate the variation in trunk bark magnetism of urban trees at large spatial
105 scale (i.e. in cities across the European continent), at local scale (i.e. within cities) and microscale (i.e.
106 within trees), in relation with levels of exposure to PM and genera. Therefore, the tree trunk bark from
107 39 genera was sampled in over 170 urban green areas (UGAs) in six European cities and analysed
108 magnetically for the SIRM. A multiple-city approach has the advantage of including multiple different
109 environmental and human-induced conditions. Particulate matter source abundance (e.g. surface area
110 of roads), measured and modelled ambient PM concentration, time of exposure, and orientation of
111 the sampled trunk were considered as indicators of PM exposure. The following research questions
112 were addressed: (1) Does trunk bark SIRM differ between cities in accordance with their mean
113 atmospheric PM concentrations? (2) Is the variation in trunk bark SIRM related to differences in tree
114 genus and does it influence the capacity of trunk bark SIRM to differentiate between cities regarding
115 PM? (3) Is variation in SIRM related to difference in levels of PM exposure, as indicated by modelled
116 atmospheric PM concentration, land use (to quantify PM source abundance), tree diameter (as an
117 indicator of time of exposure) and trunk side (orientation)? (4) What are the potential, drawbacks and
118 advantages of magnetic analysis of tree trunk bark to discriminate between sites with different PM
119 concentrations? We expect to see higher SIRM values on tree trunk bark in cities with worse air quality
120 (i.e. higher PM concentrations), in areas with more PM sources, in trees with a greater trunk
121 circumference (as indicator of tree age and as such exposure time) and at trunk sides oriented towards
122 the prevailing wind direction (more PM deposition due to greater chance of wet bark from rain and
123 increased impaction of particles from the air flow approaching the tree trunk).

124

125 **2. Methods**

126 *2.1. Sampling locations*

127 For this research, samples were collected in six European cities in the framework of the BiodivERsA
 128 project 'BIOVEINS - Connectivity of green and blue infrastructures: living veins for biodiverse and
 129 healthy cities'. These cities included Antwerp, Belgium; Lisbon, Portugal; Paris, France; Poznan, Poland;
 130 Tartu, Estonia and Zurich, Switzerland (Table 1, Fig. S1 in supplementary information (SI)). The study
 131 encompassed small cities with moderate population density and relatively low PM_{2.5} concentrations,
 132 such as Tartu, as well as large cities with high population density (e.g. Paris) or high PM_{2.5}
 133 concentrations (e.g. Poznan). Three climate types are covered in this study, i.e. temperate (Antwerp,
 134 Paris, Poznan and Zurich), Mediterranean (Lisbon) and continental (Tartu). Long-term mean yearly
 135 precipitation amounts vary between 529 and 1200 mm. The prevailing wind directions are dominated
 136 by northwest to southwest winds except for the southeasterly winds prevailing in Zurich.

137 *Table 1. Summary of cities with their abbreviation (abb.), coordinates, mean annual concentration of fine particulate matter*
 138 *in µg/m³ for 2019 and 2020 (PM_{2.5}, EEA 2021), population density (inhabitants/km² in 2018 (Eurostat 2021)), prevailing wind*
 139 *direction (WD, Meteoblue 2021), mean annual precipitation (in mm; reference period An: 1991-2020 (KMI 2021), Lx: 1991-*
 140 *2018 (IPMA 2021), Pa: 1981-2010 (Météo-France 2021), Po: 1991-2020 (Climate Change Knowledge Portal 2021), Ta: 2016-*
 141 *2020 (Estonian Weather Service 2021), Zu: 1991-2020 (MeteoSwiss 2021), climatic zone according to the Köppen – Geiger*
 142 *climate classification (Kottek et al. 2006; Cfb: temperate maritime climate, Csa: warm Mediterranean climate, Dfb: moderate*
 143 *continental climate with precipitation throughout the year) and number of sampled trees of the four main genera (Acer,*
 144 *Fraxinus, Quercus, Tilia) and all other genera with at least 10 trees sampled (Aesculus, Catalpa, Fagus, Juglans, Populus,*
 145 *Robinia, Schinus, Ulmus). *Some UGAs were located outside the Paris city center where population density might be lower.*

city	abb.	coordinates	PM _{2.5}	pop. dens.	WD	prec.	climate	Acer	Fraxinus	Quercus	Tilia	other
Antwerp	An	51° 15' 36.7"N 4° 24' 10.0"E	12.52	1,094	SW	853	Cfb	24	9	38	22	22
Lisbon	Lx	38° 43' 20.1"N 9° 8' 21.6"W	9.47	1,011	NW	815	Csa	5	6	2	2	9
Paris	Pa	48° 51' 23.8"N 2° 21' 8.0"E	10.52	21,070*	SW	638	Cfb	21	12	11	17	60
Poznan	Po	52°24'23.0"N 16°55'30.6"E	17.17	2,089	WSW	529	Cfb	63	6	7	28	18
Tartu	Ta	58°22'40.9"N 26°43'42.6"E	5.18	14	SW	690	Dfb	17	2	10	40	19
Zurich	Zu	47°22'36.8"N 8°32'30.1"E	8.59	915	SSE	1200	Cfb	37	8	24	18	36

146

147 *2.2. Experimental set-up and sampling*

148 In each city, the aim was to select 36 urban green areas (UGAs) based on their size and connectivity in
 149 the urban matrix according to the Urban Atlas 2012, as described in detail by Villarroja-Villalba et al.

150 (2021). The Urban Atlas 2012 was developed by the EU's Copernicus Land Monitoring Service based
151 on satellite image interpretation at 2.5 m resolution for the reference year 2012 (freely accessible at
152 <https://land.copernicus.eu/>). The Proximity Index (PI) was used to calculate the connectivity of UGAs.
153 It considered the area of and distance to nearby patches (radius of 5 km) with favourable habitat
154 (patches with a high probability of having trees). All possible UGAs were divided into six size and six PI
155 classes, giving 36 possible combinations. Those combined classes were used to do a random stratified
156 sampling. In the end we were able to perform sampling in 173 UGAs, of which 34 in Antwerp, 12 in
157 Lisbon, 36 in Paris, 34 in Poznan, 22 in Tartu and 35 in Zurich.

158 Inside each selected UGA, four trees, preferably of the same species, were selected in the four main
159 wind directions around the centroid of the UGA. The centroid was predetermined as the centre of
160 gravity of the UGA. When there were no four suitable trees available inside the UGA, trees were
161 selected outside the UGA but as close to the UGA as possible. The genus of each sampled tree was
162 identified in the field. Trees preferably had a diameter between 20 cm and 80 cm to avoid young and
163 very old trees and as such to ensure, as much as possible, uniformity in trunk bark structure within
164 genera. We expected variation in PM accumulation on the tree trunks due to influence of wind and
165 rain according to their prevailing direction and the position of PM sources relative to the trees. Since
166 these are expected to be tree-specific and difficult to determine accurately for each tree, particularly
167 for trees inside UGAs, we opted for uniformity and chose to collect bark at two fixed, opposite sides,
168 i.e. the north- and south-facing sides of the trunk, from here on mentioned as N- and S-facing sides.
169 Samples were taken at a height of 1.5 m above ground level using a stainless steel knife, by scraping
170 off the surface of the trunk. The bark scrape was intercepted with a plastic kidney dish, stored in a
171 labelled paper bag and transported to the lab. Tree stem circumference was measured using a
172 measuring tape at a height of 1.5 m above the ground. The knife and kidney dish were cleaned between
173 the collection of different samples.

174 The sampling campaigns were performed sequentially in Antwerp (2 – 11 May 2018), Zurich (3 – 16
175 July 2018), Poznan (19 – 28 July 2018), Tartu (25 – 26 July and 3 – 14 September 2018), Paris (22 August
176 – 2 September 2018) and Lisbon (11 May – 9 June 2019). In total, 1382 samples were collected from
177 684 trees of 39 genera in and around 173 UGAs. Four genera were sampled in all cities, i.e. *Acer*, *Tilia*,
178 *Quercus* and *Fraxinus*, which together encompassed 429 trees. It should be kept in mind that,
179 throughout this manuscript, data of a genus do not represent all species within the genus but yet
180 reflect the data of several but not all unidentified species in the genus.

181 2.3. Sample preparation and magnetic analysis

182 Before storage, samples were dried at room temperature for at least a week in the lab. From each bark
183 sample, a subsample (with median mass of 617 mg) was taken and weighed using an electronic balance
184 with an accuracy of 0.0001 g. This subsample was thoroughly packed in cling film, to avoid movement
185 of the bark, and pressed into a plastic sample pot with a volume of $6.7 \cdot 10^{-6} \text{ m}^3$. For magnetising the
186 subsample, we followed the protocol described by Kardel et al. (2011). We used a pulsed DC magnetic
187 field of 0.8 T to magnetise the subsample with the Molspin pulse magnetiser (Molspin Ltd, UK). The
188 volume magnetisation of the subsample was measured immediately after magnetisation using a JR-6
189 magnetometer with a sensitivity of 10^{-8} A m^{-1} (AGICO, Czech Republic), as the average of two
190 measurements. Method blanks were included as sample pots with the same amount of cling film as
191 was used to pack the subsamples. The obtained volume magnetisation values (in A m^{-1}) were
192 multiplied by the volume of the sample pot to obtain the magnetic moment (A m^2). The magnetic
193 moment was normalised by dividing by the mass of the subsample, which resulted in the mass-
194 normalised saturation isothermal remanent magnetisation (SIRM) expressed as $\text{A m}^2 \text{ kg}^{-1}$. Samples
195 were weighted and magnetically analysed between August 2018 and December 2019.

196 2.4. Land-use classification

197 Land-use classes in the neighbourhood of the UGAs were extracted from the Urban Atlas (UA)
198 (Copernicus Land Monitoring Service 2012) within a buffer of 200 m radius around the centroid of the
199 UGA. Land use categories were selected and combined into land-use classes to represent potential
200 sources of PM: agricultural area (UA categories 21000, 22000, 23000), urban area (UA categories
201 11100, 11210, 11220, 11230, 11240), roads (UA categories 12210, 12220), industrial area (UA
202 categories 12300, 13100, 13300) and railways (UA category 12230). Land-use categories with a
203 possible sink capacity for PM are combined in the land-use class green area (UA categories 14100,
204 14200, 31000, 32000). The area in square meters was calculated for each one of the six combined land-
205 use classes in each buffer area of 200 m radius to represent the cover of this land-use class in the
206 vicinity of the UGA.

207 2.5. Statistical analysis

208 2.5.1. City, genus and PM exposure

209 To make the dataset more balanced, we only worked with data from genera for which we had at least
210 20 samples throughout all cities. This resulted in a dataset with 1178 observations from 593 trees of
211 12 genera in 164 UGAs, further called the full 12-genera dataset (number of samples $N = 228$ in
212 Antwerp; 48 in Lisbon; 242 in Paris; 243 in Poznan; 175 in Tartu and 242 in Zurich). These 12 genera
213 were: *Acer* ($N = 332$), *Tilia* ($N = 254$), *Quercus* ($N = 180$), *Aesculus* ($N = 86$), *Fraxinus* ($N = 86$), *Populus*
214 ($N = 72$), *Robinia* ($N = 46$), *Fagus* ($N = 32$), *Catalpa* ($N = 24$), *Juglans* ($N = 22$), *Schinus* ($N = 22$) and *Ulmus*

215 (N = 22). The median circumference of the sampled trees was 129 ± 51 cm. Striking was the significantly
216 higher circumference for Tartu trees (170 ± 48 cm). Because the SIRM data were right-skewed, we In-
217 transformed them before analysis. The covers of each of the six combined land-use classes were tested
218 for correlation using the Spearman correlation test and only significantly uncorrelated PM sources
219 were used to investigate whether variation in bark SIRM can be explained by the land-use class covers
220 (PCA, Fig. S2 in SI). A mixed model was built with UGA-ID and tree-ID as random factors, with the latter
221 nested in the first, and city (factor, 6 levels), orientation (factor, 2 levels), genus (factor, 12 levels), tree
222 circumference (continuous), cover of industrial area (continuous), cover of roads (continuous) and
223 their two-way interactions as fixed factors. This model was optimised stepwise for random and fixed
224 factors based on the comparison of the Akaike Information Criterion (AIC). Model diagnostic plots were
225 checked. P values of fixed effects were obtained with the function ANOVA.

226 In the next step, to gain better insight on the possible interactions of the explanatory variables with
227 the genus effect, we focused on the four genera that occurred in all of the six cities, namely *Acer*, *Tilia*,
228 *Quercus* and *Fraxinus*. These four genera represent 72% of the full 12-genera dataset (Table 1) and is
229 further on called the 4-genera dataset ($N_{\text{total}} = 852$: $N_{\text{Antwerp}} = 185$; $N_{\text{Lisbon}} = 30$; $N_{\text{Paris}} = 122$; $N_{\text{Poznan}} = 207$;
230 $N_{\text{Tartu}} = 138$; $N_{\text{Zurich}} = 170$). Hereon, we applied and optimized a similar mixed model as above with only
231 four levels for the variable genus.

232 Next, we investigated the relationship of SIRM values with PM exposure at city level, taking the city-
233 specific mean annual measured $\text{PM}_{2.5}$ concentrations of 2019-2020 (Table 1) as indicator. A mixed
234 model was built to evaluate influence of the mean annual $\text{PM}_{2.5}$ concentration at city level on the SIRM
235 values and taking into account genus, circumference, tree trunk side and cover of industry and roads.
236 This was done for both the 12-genera and the 4-genera dataset. *Acer* was the only genus that was
237 represented in each city with at least five trees. Therefore, at city level, the correlation between
238 median bark SIRM values of *Acer* with 2-year-mean annual PM concentrations was tested with a
239 Pearson correlation test (N = 6).

240 2.5.2. Correlation of modelled PM data with bark SIRM values for Antwerp

241 For the locations of all trees sampled in Antwerp (N = 129), modelled PM_{10} and $\text{PM}_{2.5}$ concentrations
242 for the years 2018 and 2019 were extracted from concentration maps derived from the ATMO-Street
243 model chain (Lefebvre et al. 2013; IRCELINE 2018, 2019) using QGIS software (QGIS Development
244 Team 2020). The SIRM and the modelled PM_{10} and $\text{PM}_{2.5}$ data were right-skewed and were In-
245 transformed prior to analysis. A mixed model was built to investigate the effect of modelled PM
246 concentrations on the measured SIRM values. Orientation (factor, 2 levels), genus (factor, 12 levels),
247 tree trunk circumference (continuous) and GIS-extracted modelled PM concentrations (continuous)

248 were used as fixed factors. UGA-ID and tree-ID were used as random factors, with the latter nested in
249 the first. The same model (but without the explanatory variable “genus”) was run for subsets of the
250 three most common genera in Antwerp: *Quercus* (N = 76), *Acer* (N= 47) and *Tilia* (N = 44).

251 2.5.3. Spatial interpolation and inter-genera correlation

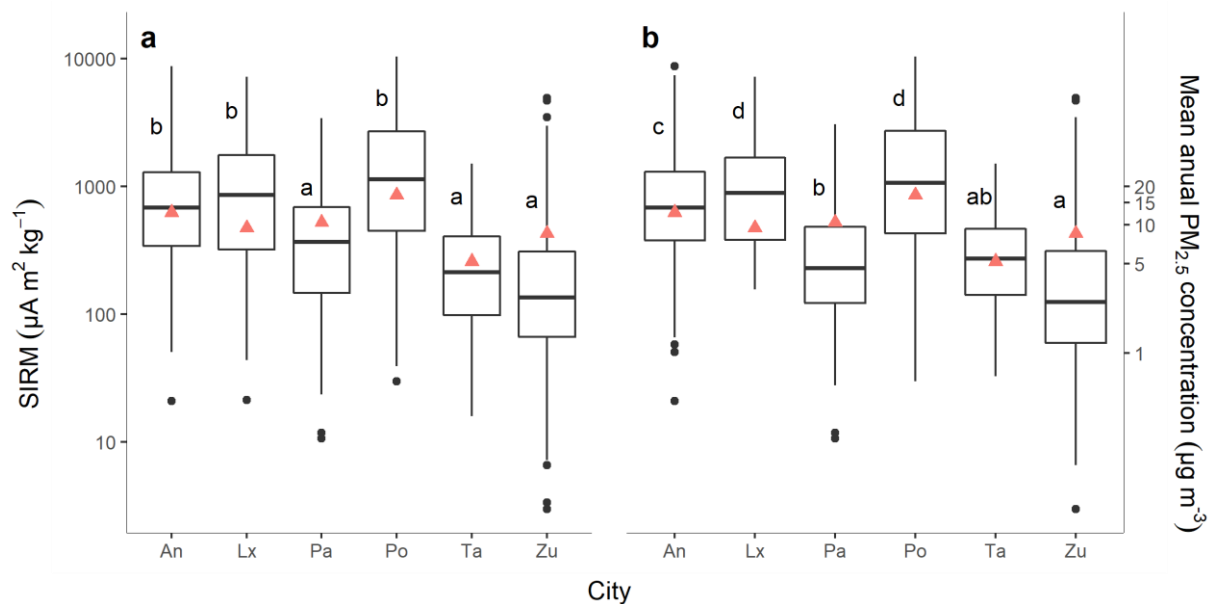
252 To investigate relations between the bark SIRM values of the different genera, spatial interpolation
253 was performed at city level for *Acer* data (the most sampled genus) for the cities with sufficient
254 coverage of *Acer* trees: Antwerp (N = 24), Poznan (N = 63) and Zurich (N = 37). Interpolation was done
255 on the mean values per *Acer* tree (i.e. mean of N and S samples) using QGIS (QGIS Development Team
256 2020). After this, the SIRM values for *Acer* were extracted from the interpolated maps at the locations
257 of the trees from the two other abundant genera *Tilia* and *Quercus* in Antwerp ($N_{Tilia} = 15$, $N_{Quercus} =$
258 20), Poznan ($N_{Tilia} = 17$, $N_{Quercus} = 6$) and Zurich ($N_{Tilia} = 18$, $N_{Quercus} = 24$). The Pearson correlation test
259 was used on the ln-transformed data to check for correlations between the interpolated SIRM values
260 of genus *Acer* and the mean measured SIRM values of *Tilia* and *Quercus* (i.e. the mean of samples at
261 N- and S-sides of the tree). All statistical analyses were performed in R 4.1.2 (R Core Team 2021). The
262 linear mixed models were built on ln-transformed SIRM data using the package nlme (Pinheiro et al.
263 2021). Images were made using the package ggplot2 (Wickham 2016). In all statistical tests, p-values \leq
264 0.05 were considered as significant.

265 3. Results

266 3.1. City, genus and PM exposure: the 12-genera dataset

267 The tree trunk bark SIRM value ranged between 3.0 and 10346.6 $\mu\text{A m}^2 \text{kg}^{-1}$ over the six cities and 12
268 genera (i.e. those with at least 20 samples), with a median value of 406.2 $\mu\text{A m}^2 \text{kg}^{-1}$. Genera to climate
269 relationships were observed e.g., *Catalpa* and *Juglans* were only represented in the southern cities.
270 According to the mixed model, with UGA-ID and tree-ID as nested random factors, city ($p < 0.0001$),
271 genus ($p < 0.0001$), circumference ($p < 0.0001$), orientation ($p = 0.0009$), cover of industrial area ($p =$
272 0.0028) and cover of roads ($p = 0.0011$) contributed significantly to the variation in bark SIRM of the
273 12 genera. There was a significant interaction between city and circumference ($p = 0.0063$), city and
274 orientation ($p < 0.0001$), city and cover of industrial area ($p = 0.0038$, Fig. S3 in SI) and between city
275 and cover of roads ($p < 0.0001$, Fig. S3 in SI). The lowest SIRM values occurred in Zurich, while the
276 highest values were observed in Poznan (Fig. 1). The median SIRM values of the bark including the 12
277 genera increased in the following order: Zurich, Tartu, Paris, Antwerp, Lisbon, Poznan. The SIRM values
278 were significantly higher in Antwerp, Lisbon and Poznan than in Paris, Tartu and Zurich.

279
280



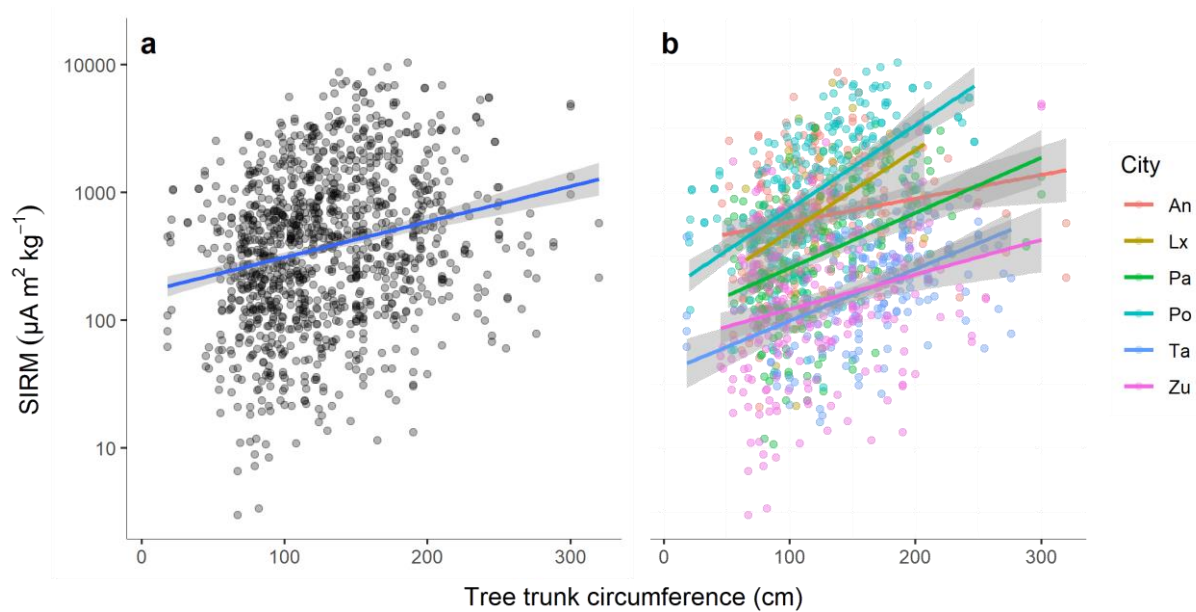
281

282 **Fig. 1** Median and quantile normalised SIRM values of tree trunk bark for the 12-genera dataset (a) and the 4-genera dataset
283 (b) for the six cities under investigation (An= Antwerp, Lx = Lisbon, Pa = Paris, Po = Poznan, Ta = Tartu, Zu = Zurich; 12-genera
284 dataset: $N_{An} = 228$, $N_{Lx} = 48$, $N_{Pa} = 242$, $N_{Po} = 243$, $N_{Ta} = 175$, $N_{Zu} = 242$; 4-genera dataset: $N_{An} = 185$, $N_{Lx} = 30$, $N_{Pa} = 122$, $N_{Po} =$
285 207 , $N_{Ta} = 138$, $N_{Zu} = 170$). The horizontal lines represent Q1, median and Q3. SIRM values can be read off from the left y-axis.
286 Different letters indicate significant differences in SIRM values between the cities according to the mixed model outcome. Red
287 triangles represent the, mean annual concentration of fine particulate matter in $\mu\text{g}/\text{m}^3$ for 2019 and 2020 ($\text{PM}_{2.5}$, EEA (2021))
288 as shown in Table 1 and values can be read off from the right y-axis. Mind the logarithmic scale of the y-axes.

289

290 The SIRM varied significantly between the genera (overview in Fig. S4 in SI). Taking into account the
291 variation caused by city and tree circumference, the lowest values occurred in *Fagus*, intermediate
292 values (in order of increasing values) in *Populus*, *Fraxinus*, *Acer*, *Catalpa*, *Quercus*, *Ulmus*, *Tilia*, *Aesculus*
293 and *Juglans*, and the highest values (in order of increasing values) in *Robinia* and *Schinus*.

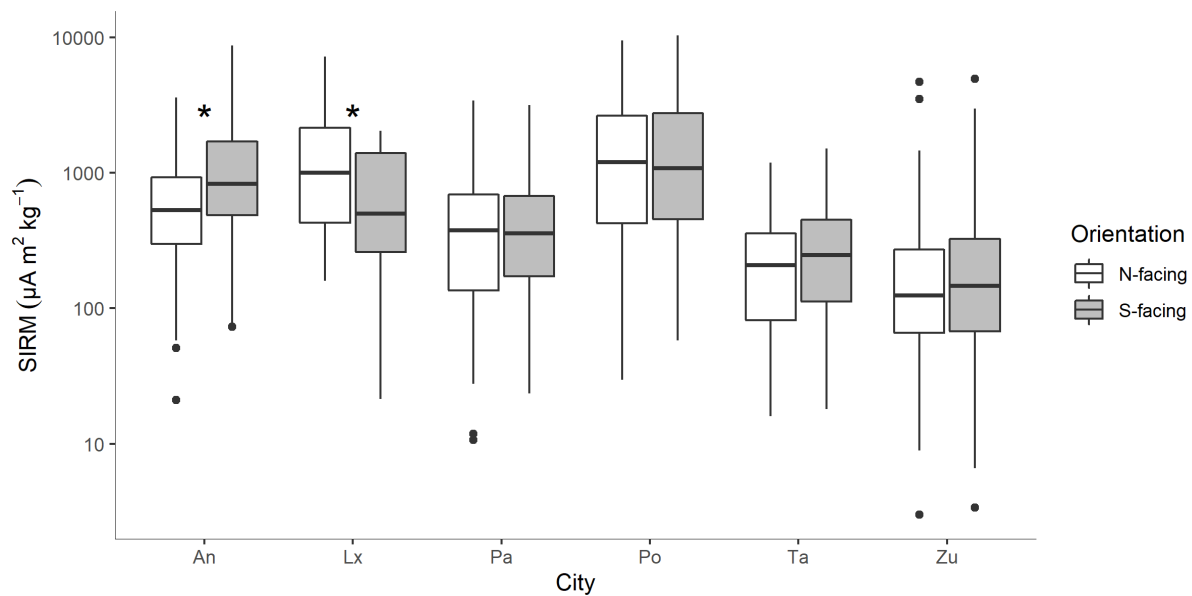
294 In all cities, the bark SIRM significantly increased with increasing circumference (Fig. 2a), following a
295 linear relationship between the ln-transformed bark SIRM and the tree circumference and thus the
296 tree trunk bark SIRM values increased exponentially with tree circumference. However, there was a
297 significant interaction effect between circumference and city. The trend lines were significantly
298 steeper for Paris and Poznan than for Antwerp, Tartu and Zurich (Fig. 2b).



300

301 **Fig. 2** Normalised SIRM values of tree trunk bark in function of tree trunk circumference for all cities (a) and for the six studied
 302 cities individually (b) (An = Antwerp, Lx = Lisbon, Pa = Paris, Po = Poznan, Ta = Tartu and Zu = Zurich). Given the logarithmic
 303 scale of the y-axis, there is an exponential trend of increasing SIRM values with expanding tree trunk circumference at a height
 304 of 1.5 m above ground plotted with `geom_smooth`. Grey bands show the 95% confidence interval.

305 In general, the SIRM values at the N-facing side of trees were lower than at the S-facing side of trees
 306 ($p < 0.0001$) but there was a significant interaction between orientation and city ($p < 0.0001$). In
 307 Antwerp, the S-facing bark had significantly higher SIRM values ($p < 0.0001$), while in Lisbon, the SIRM
 308 of the N-facing bark was higher ($p = 0.0002$). In Antwerp, the median at the N-facing side was 35 %
 309 lower than at the S-facing side. In Lisbon, the SIRM median values at the N-facing side were double of
 310 those on the S-facing side. In Paris, Poznan, Tartu and Zurich, no significant differences occurred in
 311 bark SIRM between N and S orientation (Fig. 3).



313

314 **Fig. 3** Normalised SIRM values at the north (N)- and south (S)- facing sides of the sampled trees. Results are shown for the 12
 315 genera for which at least 10 trees were sampled in the six studied cities (An = Antwerp, Lx = Lisbon, Pa = Paris, Po = Poznan,
 316 Ta = Tartu and Zu = Zurich). Asterisk shows cities with significant differences between both sides ($* = p \leq 0.05$). Mind the
 317 logarithmic scale of the y-axis.

318 The cover of roads and cover of industry were not significantly correlated ($r = 0.07$, $p = 0.3885$) and
 319 contributed both to the variation in SIRM. The cover of industrial area in the buffer zones did
 320 significantly correlate with the cover of urban area ($r = -0.34$, $p < 0.0001$), agriculture ($r = -0.22$; $p =$
 321 0.0038) and railways ($r = 0.15$, $p = 0.0532$). The cover of industrial area and roads around the UGA
 322 centroid had a positive significant effect on the SIRM values, but these effects were city-dependent.
 323 The SIRM values increased significantly more per unit surface increase of industrial area in Zurich than
 324 in Antwerp, Lisbon and Paris. The least steep relationship between the SIRM value and cover of
 325 industrial area was found in Paris; only in Tartu and Zurich, this relationship was significantly steeper.
 326 Also for the cover of roads, there was an interaction with the city effect: the SIRM values increased
 327 more with an increasing cover of roads in Poznan, Zurich and Paris than they did in Lisbon and Antwerp.

328 3.2. City, genus and PM exposure: the 4-genera dataset

329 When considering only the four genera that occurred in all of the six cities, namely *Acer* ($N = 332$), *Tilia*
 330 ($N = 254$), *Quercus* ($N = 180$) and *Fraxinus* ($N = 86$), the SIRM values ranged between 3.0 and 10346.6
 331 $\mu\text{A m}^2 \text{kg}^{-1}$ over the six cities and four genera (i.e. those that occur in all cities), with a median value of
 332 $412.1 \mu\text{A m}^2 \text{kg}^{-1}$. The optimised mixed model, with UGA-ID and tree-ID as nested random factors,
 333 indicated a significant contribution of city ($p < 0.0001$), genus ($p = 0.0004$), circumference ($p < 0.0001$),
 334 orientation ($p = 0.0019$), cover of roads ($p = 0.0036$) and cover of industrial area ($p = 0.0085$) to the
 335 variation in bark SIRM, with a significant interaction between city and orientation ($p = 0.0001$), city and

336 cover of roads ($p = 0.0003$) and city and cover of industrial area ($p = 0.0117$). The lowest SIRM values
337 occurred in Zurich, while the highest values were observed in Poznan (Fig. 1). The median values of the
338 bark SIRM including the four genera increased in the following order: Zurich, Paris, Tartu, Antwerp,
339 Lisbon, Poznan.

340 The lowest SIRM values were for samples of the genera *Fraxinus* and *Acer*, while the genus *Quercus*
341 had intermediate values and the values for *Tilia* samples were significantly higher than those of *Acer*
342 ($p = 0.0018$) and *Fraxinus* ($p = 0.0298$) (overview in Fig. S4 in SI). Moreover, a significant increase in
343 SIRM values was observed with tree circumference ($p < 0.0001$), irrespective of genus and city. In
344 general, significantly higher SIRM values were observed at the S-facing side of the tree, as opposed to
345 the N-facing side of the trees ($p < 0.0001$), but there was a significant interaction between city and
346 orientation ($p = 0.0001$). There were significant differences between samples from N- and S-facing side
347 of trees in Antwerp and Lisbon. In Antwerp, the median at the N-facing side was 34 % lower than at
348 the S-facing side. In Lisbon, the opposite was true with median values at the N-facing side that were
349 more than three times as high (314 %) as those on the S-facing side.

350 The covers of industrial area and roads in the vicinity of the UGAs had a positive significant effect on
351 the SIRM values, but these effects were city-dependent. As with the 12-genera dataset, the SIRM
352 values increased significantly more per surface of industrial area in Zurich than in Antwerp, Lisbon and
353 Paris. The least steep relationship between SIRM value and cover of industrial area was found in Paris,
354 only in Tartu and Zurich this relationship was significantly steeper. Also the cover of roads, interacted
355 significantly with the city effect: SIRM values increased more with an increasing cover of roads in
356 Poznan, Zurich and Paris than in Antwerp. In Tartu, the increase in SIRM values with cover of roads was
357 significantly lower than in Paris, but did not significantly differ from the other cities.

358 3.3. Relationships of SIRM values with PM data

359 Following the mixed models outcome in which the circumference, genus, tree side and land-use classes
360 were accounted for, the cities' mean annual measured $PM_{2.5}$ concentration contributed significantly
361 to the variation in SIRM, for both the 12-genera ($p < 0.0001$) and the 4-genera ($p < 0.0001$) dataset.
362 Positive relationships between the annual measured $PM_{2.5}$ concentration and the SIRM were observed.
363 Moreover, the six median bark SIRM values of *Acer* – the only genus with at least five trees in each city
364 – correlated significantly and positively with the cities' mean annual measured $PM_{2.5}$ concentrations (r
365 $= 0.91$, $p = 0.0124$, Fig. S5 in SI).

366 For the detailed analyses in Antwerp, the modelled PM_{10} and $PM_{2.5}$ concentrations were correlated (in
367 each year 2018 and 2019: $p < 0.0001$) and so were the PM concentrations of the different years 2018
368 and 2019 (in each size fraction $PM_{2.5}$ and PM_{10} : $p < 0.0001$). For this reason, only one series of data for

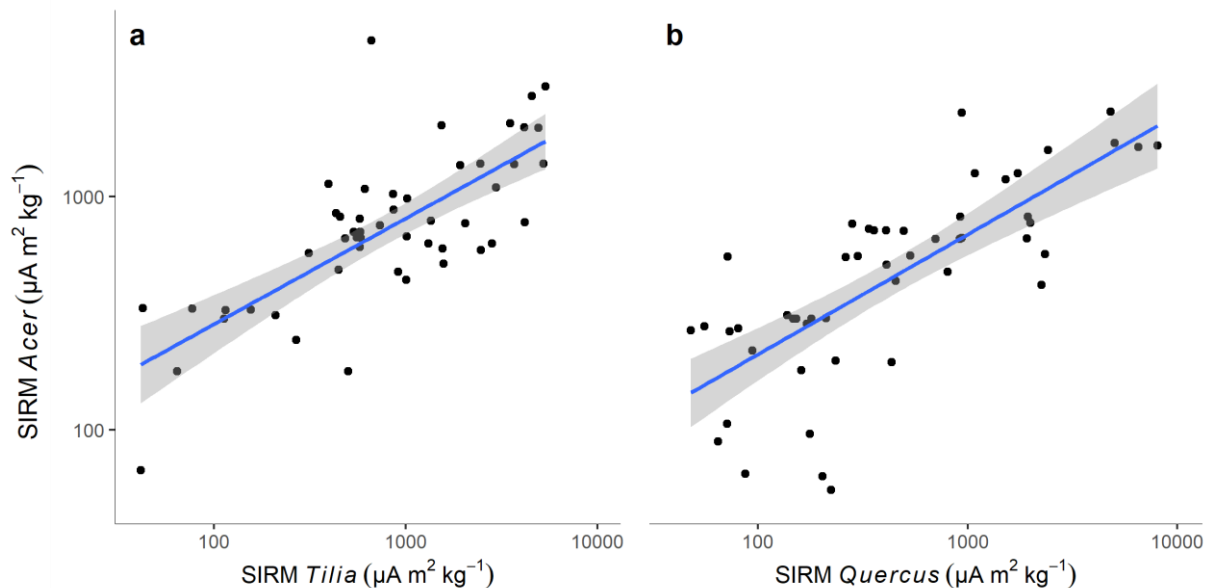
369 PM concentrations was kept in the model at the same time. For none of the years and fractions did
370 the modelled PM concentration at the sampling locations contribute to the explanation of the variation
371 in SIRM values ($PM_{2.5, 2018}$: $p = 0.9033$; $PM_{10, 2018}$: $p = 0.9451$; $PM_{2.5, 2019}$: $p = 0.9125$; $PM_{10, 2019}$: $p = 0.7716$).
372 For all of the three subsets of the most common genera in Antwerp, the same conclusions could be
373 drawn.

374 3.4. Inter-genera correlation

375 There was a significant correlation between the SIRM values for *Tilia* trees (averaged at tree level) and
376 the interpolated SIRM values for genus *Acer* extracted at the *Tilia* tree location ($r = 0.74$, $p < 0.0001$).
377 Similarly, the SIRM values for trees of the genus *Quercus* were significantly correlated with the
378 interpolated SIRM values for *Acer* extracted at the *Quercus* tree locations ($r = 0.75$, $p < 0.0001$). The
379 relationship between these values is described by the linear relationships $SIRM_{Acer} = 0.3 * SIRM_{Tilia} +$
380 531.5 and $SIRM_{Acer} = 0.2 * SIRM_{Quercus} + 394.5$ (Fig. 4, Fig. S6 in SI).

381

382



383

384 **Fig. 4** Relationship between the spatially interpolated SIRM values for *Acer* trees at the locations of *Tilia* (a; $y = 0.3 * x + 531.5$,
385 $R^2_{adj} = 0.54$, $p < 0.0001$) and *Quercus* (b; $y = 0.2 * x + 394.5$, $R^2_{adj} = 0.56$, $p < 0.0001$) trees. The SIRM-values of *Acer* were extracted
386 from the interpolation maps in Fig. S6 in SI for cities Antwerp, Poznan and Zurich. Grey bands indicate the 95% confidence
387 interval.

388 4. Discussion

389 This study is the first to study tree bark SIRM on a continental scale, in different climate zones, in
390 different urban settings and with a large variety of genera. Our results indicate the importance of
391 surrounding land use, genus, tree circumference and orientation resulting in differences in bark SIRM

392 related to PM exposure. The median tree trunk bark SIRM value of $406.2 \mu\text{A m}^2 \text{kg}^{-1}$ obtained in this
393 study falls within the range of SIRM values for bark found by Hofman et al. 2017 (4.3 to $2980 \mu\text{A m}^2 \text{kg}^{-1}$)
394 and Kletetschka et al. 2003 (270 to $1530 \mu\text{A m}^2 \text{kg}^{-1}$ in Goddard, Maryland, US), but is lower than the
395 range of 2500-19200 $\mu\text{A m}^2 \text{kg}^{-1}$ observed by Chaparro et al. (2020) in Mar del Plata in Argentina.
396 Moreover, a large range with SIRM values up to $10346.6 \mu\text{A m}^2 \text{kg}^{-1}$ was observed in this study. This
397 large variation in SIRM value here is probably the result of the large extent of the study, including a
398 large sample size in different urban settings and climate zones, and the large variation in factors that
399 influence the bark SIRM value, i.e. tree genus, tree circumference and site- and city specific PM
400 exposure.

401 *4.1. Inter-city variations in SIRM*

402 The trunk bark SIRM differed between cities, with higher values in Poznan, Lisbon and Antwerp and
403 lower values in Paris, Tartu and Zurich (Fig. 1). This is in line with the higher recent mean annual
404 concentrations of $\text{PM}_{2.5}$ measured in Antwerp and Poznan and the lower $\text{PM}_{2.5}$ concentrations for Tartu
405 and Zurich (Table 1, Fig. 1), in spite of the difference in time span represented by bark SIRM (which
406 increases with tree age (see §4.4.2) and thus can be considered a time-integrated PM proxy) and the
407 recent $\text{PM}_{2.5}$ concentrations. However, Paris and Lisbon seem to deviate slightly from this similarity:
408 trees in Paris had lower bark SIRM and those in Lisbon higher SIRM values than could be expected
409 based on the mean annual $\text{PM}_{2.5}$ concentrations. In Paris, site selection included parks outside the city
410 center and sometimes in low urbanised landscape far away from the most urbanised sites; this can
411 explain SIRM values being lower than expected from the city's mean annual $\text{PM}_{2.5}$ concentration. In
412 Lisbon, sampling was performed one year later than in the other cities, which may have contributed
413 to higher SIRM values than expected, although this effect is expected to be marginal. Nonetheless, the
414 measured $\text{PM}_{2.5}$ concentrations can significantly explain variation in SIRM at city level when the
415 influence of genus, circumference, tree trunk side and the cover of roads and industry are controlled
416 for. The tree trunk SIRM increased with increasing levels of mean annual $\text{PM}_{2.5}$ concentrations. More
417 specifically, when only SIRM values of *Acer* were considered, i.e. the only genus with at least five trees
418 sampled per city, also a significant and positive correlation was observed between the cities' mean
419 annual measured $\text{PM}_{2.5}$ concentrations and their median bark SIRM. Our results confirm that trunk
420 bark SIRM differs between cities in accordance with their mean atmospheric PM concentrations
421 (research question 1).

422 When considering the four genera that occurred in all cities, the interaction between city and genus
423 was not significant, so the differentiating power of bark SIRM between cities with different $\text{PM}_{2.5}$ levels
424 was similar for each of the considered genera. We conclude that the power of trunk bark SIRM to

425 differentiate between cities according to their mean annual PM concentration is irrespective of the
426 four widespread genera considered in this study (research question 2).

427 4.2. Inter-tree variation in SIRM

428 4.2.1. PM sources in tree surroundings

429 Across the six cities, the bark SIRM values were found to increase with increasing covers of industrial
430 area and of roads in the surroundings of the UGAs. These results indicate the sensitivity of bark SIRM
431 to magnetic PM emissions from industrial activities and traffic. Elevated SIRM signals in industrial areas
432 and closer to roads with motorised traffic opposed to green areas have been observed previously for
433 leaves (Hansard et al. 2011; Castanheiro et al. 2016; Kardel et al. 2012; Moreno et al. 2003), the bark
434 of tree branches (Wuyts et al. 2018) and tree trunk bark (Brignole et al. 2018). This study, nonetheless,
435 goes beyond the categorical comparison of land use classes and is, to our knowledge, the first to
436 identify a relationship between tree trunk bark SIRM and the cover of industrial area and roads in the
437 vicinity of the sampling location, and thus to quantitatively generalise the influence of land use on
438 SIRM (research question 3).

439 Furthermore, the interactions of the city effect with the cover of industrial area and with the cover of
440 roads suggest that the effect size of road and industry cover on bark SIRM was city-specific. As amount,
441 chemical composition and size fraction distribution of deposited PM influence its SIRM signal (Hofman
442 et al. 2014a; Castanheiro et al. 2021), these interactions imply that industrial areas and roads in
443 different cities emit magnetic PM in different amounts per surface area and/or in other chemical
444 composition or size fraction distribution. Indeed, studies by Sawidis et al. (2011) on accumulated
445 metals in tree bark and by Baldacchini et al. (2017) on PM on leaves at street sites found different
446 chemical compositions across European cities. These differences were attributed to differences in PM
447 sources, i.e. local geochemistry, population density, the type and location of industrial activities and
448 traffic, and the rate of technological innovations and emission control programs. We, therefore
449 recommend further research to look into the potential of tree trunk bark SIRM to differentiate
450 between different source types, whether or not in combination with chemical analyses (Lopes Moreira
451 et al. 2016).

452 4.2.2. Modelled PM concentrations

453 Bark SIRM values did not significantly correlate with the modelled PM₁₀ and PM_{2.5} concentrations in
454 Antwerp city. This is in line with the findings of Hofman et al. (2014b) who saw a bad agreement
455 between SIRM values of ivy (*Hedera sp.*) leaves and modelled atmospheric PM₁₀ concentrations. Using
456 measured PM concentrations, however, Mitchell and Maher (2009) did find a strong correlation
457 between leaf SIRM values and pumped air filter particulate mass. The disagreement between the

458 modelled PM₁₀ and PM_{2.5} concentrations and the bark SIRM values in our study can be explained by
459 the time range during which PM has been accumulating on the sampled bark. When samples are
460 collected from 50-year-old trees, they have been subjected to PM concentrations in the air at that
461 specific location for all those years. The modelled PM₁₀ and PM_{2.5} concentrations from the previous
462 years are likely not representative of the PM exposure in the lifespan of the trees. Moreover,
463 inaccuracies in the PM model outcomes are plausible due to limited or inaccurate input data (e.g.
464 limited number of measuring stations and uncertainty in emission data), model assumptions and local
465 and temporary conditions (Lefebvre et al. 2013). Also, in a mixed-source environment, variation in
466 SIRM reflects not only differences in atmospheric PM₁₀ or PM_{2.5} concentrations but also in composition
467 and magnetic grain size, since different PM sources may induce different leaf SIRM values at
468 comparable Fe content or atmospheric PM mass concentration (Baldacchini et al. 2017, Hansard et al.
469 2011). This was also pointed out by the different relationships between bark SIRM and the cover of
470 roads and industrial land use (§4.2.1). Our SIRM data were capable of capturing the high spatial
471 variation in PM exposure typical of urban settings, both in amount and composition, and can take into
472 account local conditions. Hence, we suggest measuring bark SIRM values to get a better idea of the
473 spatial variation in anthropogenic coarse and fine PM concentrations at a higher spatial resolution in
474 order to complement PM measurements and to be taken into account in PM concentration models,
475 preferentially in areas dominated by the same anthropogenic PM source.

476 4.2.3. Genera and bark structure

477 The bark SIRM significantly depended upon the genus of the sampled tree. Notable are the low values
478 for *Fagus* trees and high values for *Robinia* and *Schinus*. In the smaller 4-genera dataset (with genera
479 sampled in all cities) the SIRM values of the genera *Acer* and *Fraxinus* were significantly lower than
480 those for *Tilia*. Roughness of the exposed surface is a variable known to increase deposition of PM as
481 proven by Muhammad et al. (2020) for leaves, and our results suggest that it seems to play a role in
482 accumulation of PM on bark too. The sole representative of *Fagus* in Europe is *F. sylvatica*, which
483 displays a very smooth and thin bark at all ages. The genus *Acer* in this study encompassed *A.*
484 *pseudoplatanus* and *A. platanoides*, both showing a smooth bark surface at young and intermediate
485 age and a rougher bark surface only at later age (with shallow cracks and furrows, respectively). In
486 addition, since the magnetic signal of bark is confined to the outermost surface (Wuyts et al. 2018),
487 exfoliation as observed for *A. pseudoplatanus* bark scales at later age can reduce the magnetic signal.
488 The very rough, non-exfoliating bark of *Robinia pseudoacacia* (the sole representative of the *Robinia*
489 genus in this study) and the genus *Schinus* can explain their very high values of bark SIRM. The dense
490 longitudinal fissures and cracks in the bark of the *Tilia* species in this study (*T. platyphyllos*, *T. cordata*
491 and *T. tomentosa*) provide a rough surface as well, but yet with micro-roughness rather than *Robinia-*

492 like macro-roughness. It should be noted also that a thick bark may dilute the magnetic signal per mass
493 unit, as the accumulation is restricted mainly to the exposed surface (Wuyts et al. 2018). This could
494 cause underestimation of the PM accumulation on bark of species with thick bark, such as *Quercus* and
495 *Populus*. Nonetheless, rough bark surface seems to stimulate PM accumulation, but it is probable that
496 other trunk bark traits also play a role in bark PM accumulation, such as its water holding capacity and
497 wettability.

498 4.2.4. Tree circumference as a measure for exposure time

499 Tree trunk bark SIRM increased with increasing tree trunk circumference, probably via its relationship
500 with tree age. With increasing tree trunk circumference, the ln-transformed bark SIRM signal increased
501 linearly (Fig. 2), and this for all genera studied and a broad range of circumferences, i.e. between 50
502 and 300 cm. For a given PM deposition velocity on bark, it can be expected that PM accumulates on
503 bark with time, at least for trees with non-exfoliating bark, resulting in increasing PM per surface area
504 and SIRM as trees age whilst their circumference increases. In conditions with low competition for light
505 as can be expected in urban settings, tree circumference can be considered as a rough indicator of tree
506 age (Wegiel et al. 2017). According to Catinon et al. (2009), the accumulation of superficial deposits on
507 young stems of *F. excelsior* trees reaches a maximum after 10-15 years, after which the accumulation
508 per area unit of bark only slowly increases. Increasing SIRM values with tree age were also observed
509 by Wuyts et al. (2018) who investigated SIRM values of *Platanus x acerifolia* tree branches of different
510 ages. The effect of surface roughening with aging, stimulating the deposition of PM on the surface,
511 may also have played a role in the early years of tree development. It should be kept in mind that for
512 trees in urban environments tree age and exposure time may not fully coincide: urban trees are
513 brought in at variable ages and diameters from a tree nursery where they have experienced PM
514 exposure different from that at their current urban location during a period that may also vary from
515 tree to tree. The time since tree planting is therefore probably more representative of the exposure
516 time than tree diameter. The increase in SIRM values with tree trunk circumference was city-
517 dependent as not all slopes in the relationship were equally steep for each city (Fig. 2b) and a significant
518 interaction occurred between circumference and city effects. Via the relation of circumference with
519 tree age and thus exposure time, an explanation for this interaction can be found in differences in the
520 growth rate of trees and accumulation rate in the different cities. The latter, in turn, could relate to
521 differences in PM concentrations, PM size distribution and meteorology (e.g. wind speed and rain)
522 between cities. Although the effect of exposure time on tree trunk circumference is city-dependent,
523 we can conclude that tree trunk circumference will increase with tree age in all cities without reaching
524 a maximum value and this irrespective of genus.

525 4.3. Intra-tree variation in SIRM: orientation

526 Although the bark SIRM values were in general lower at the N-facing than at the S-facing side of trees
527 (Fig. 3), a significant interaction with city was observed. The SIRM values in Antwerp and Lisbon were
528 1.5-2 times higher at the side of the tree that corresponds to the prevailing wind direction (in Antwerp
529 SW and in Lisbon NW). For the other cities, the sampling sides did not coincide with the prevailing wind
530 direction, so no potential effect of prevailing wind direction could be detected. The prevailing wind-
531 facing side of trees is more likely to get wet from rain during a downpour than the other side of the
532 tree. The presence of water facilitates the deposition of PM and stickiness for particles is higher on
533 moist surfaces (Kletetschka et al. 2003), but a possibly higher wash-off at this side may also occur.
534 Moreover, the wind-facing side of trees undergoes a larger impactation of upcoming PM by the direct
535 air flow on the surface, a process which is most effective for coarse particles (Fowler et al. 2009), i.e.
536 the particles with the highest magnetic concentration (Revuelta et al. 2014).

537 4.4. Advantages and drawbacks of biomagnetic monitoring using tree trunk bark

538 In the light of research question 4, we here evaluate the potential, drawbacks and advantages of using
539 magnetic analysis of tree trunk bark to discriminate between sites with different PM concentrations,
540 based on our study's results and experience. As atmospheric PM will predominantly accumulate at the
541 outer surface of the tree (Wuyts et al. 2018), it is better to collect bark with an object that takes a small
542 and fixed surface (e.g. a corer or template). This enables the calculation of surface-normalised bark
543 SIRM, making the samples independent of bark thickness while ensuring that the entire surface is
544 sampled instead of only the protrusive bark parts. Alternatively, all samples need to be taken up to a
545 fixed and not too large depth otherwise the signal might be diluted for each species differently.
546 Moreover, we suggest to use tree species that can be sampled rather easily, i.e. species with a
547 smoother trunk (e.g. *F. sylvatica*), and avoid species with a very rough or exfoliating trunk (e.g. *Platanus*
548 *sp.*). When there is limited time or resources, and only one sample per tree can be taken, it is advised
549 to take samples according to the overall predominant wind direction as this will result in the highest
550 SIRM values with the lowest relative measuring error in areas with low air pollution. Furthermore, the
551 significant relationships between the SIRM values of *Acer-Tilia* and *Acer-Quercus* tree pairs (Fig. 4)
552 endorse the possibility of increasing the spatial sampling resolution and cover of a biomagnetic
553 monitoring study through the combination of different tree genera. SIRM values of different genera
554 are then to be rescaled to the most abundant genus with inter-genera calibration formulae. A similar
555 suggestion was made before for leaves by Kardel et al. (2011) based on a linear relationship between
556 the leaf SIRM of pairwise co-located *Tilia sp.* and *Carpinus betulus* trees.

557 Sampling trunk bark for biomagnetic monitoring has some advantages over the use of leaves and
558 branches. It can be sampled during all seasons, as opposed to leaves of deciduous species. When

559 working with leaves in temperate climates, research in winter periods is limited to evergreen species
560 which will reduce the spatial resolution of the study. Moreover, trunk bark can be sampled at breathing
561 height, which is more relevant for human PM exposure assessments. In many cases, this is a height
562 where branches and leaves are not available. When sampling leaves or branches high up in the canopy,
563 often a telemetric pruner or, even more complicated in urban settings, a crane needs to be used and
564 the chance of contamination of the samples is high. However, sampling of the tree trunk also has
565 disadvantages. In absence of a tree database with info on planting date, one cannot determine exactly
566 in an non-destructive, easy and cheap way the age of the bark and thus its exposure time. Therefore,
567 in order to use tree trunk magnetic sampling the tree trunk circumference must be controlled for either
568 during sampling or during statistical analysis. For young branches and foliage, and particularly for
569 leaves of deciduous species, surface exposure time generally is easier to assess. Moreover, preparing
570 trunk bark for magnetic analysis takes more time and effort than using branches (which can be easily
571 cut in pieces) or leaves (which can be rolled up) to fit in the plastic sample container for lab analysis.

572 **5. Conclusion**

573 The SIRM signal of trunk bark from urban trees varies greatly between and within cities, from
574 continental to tree level. Through their effect on magnetic PM accumulation on the exposed bark, tree
575 genus, cover of PM-emitting sources (i.e. roads and industry) near the tree, PM concentrations and
576 tree circumference (as an indicator of tree age) explain the variation observed in tree trunk bark. Intra-
577 tree variation occurs in relation with trunk side (orientation) relative to the prevailing wind direction.
578 We can conclude that the magnetic signal of tree trunk bark is a good proxy for ambient coarse to fine
579 PM concentrations and enables to catch variation in anthropogenic PM exposure from traffic and
580 industry at a local scale in areas dominated by the same anthropogenic PM source . However, our
581 results point to the importance of monitoring bark SIRM with a standardised sampling protocol, in
582 which genus, tree circumference (or age) and trunk side are thoughtfully selected. Nonetheless, the
583 combination of different genera in one monitoring study with bark SIRM via inter-calibration seems
584 valid and could enhance a biomonitoring study's spatial sample resolution and coverage. Therefore,
585 we can recommend the use of bark from urban trees from different genera as an easy to measure,
586 reliable and time-integrative proxy for source-specific, coarse to fine PM exposure at local scale.

587

588 **Statements & Declarations**

589 *Funding*

590 This study was supported by the Belgian Science Policy (Belspo) within the Belgian research action
591 through interdisciplinary networks (BRAIN-be) with project number BR/175/A1/BIOVEINS-BE. This

592 was within the framework of the ERA-NET BiodivERsA project 'BIOVEINS - Connectivity of green and
593 blue infrastructures: living veins for biodiverse and healthy cities' (H2020 BiodivERsA32015104). A.
594 Van Mensel, R. Samson and K. Wuyts acknowledge funding from the University of Antwerp. P. Pinho
595 acknowledges Fundação para a Ciência e a Tecnologia (FCT, 2020.03415.CEECIND). B. Muyshondt
596 acknowledges funding from a PhD grant Strategic Basic Research of the Research Foundation -
597 Flanders (FWO, 1S84819N). C. Aleixo gratefully acknowledges FCT for the financial support (PhD
598 grant reference SFRH/BD/141822/2018). M. Alos Orti was supported by the European Social Fund's
599 Dora Plus Programme. J. Casanelles-Abella was supported by the Swiss National Science Foundation
600 (project 31BD30_172467). P. Tryjanowski acknowledges the National Science Center Poland (NCN)
601 for funding through NCN/2016/22/Z/NZ8/00004.

602 *Competing interests*

603 The authors have no relevant financial or non-financial interests to disclose.

604 *Author contributions*

605 . Anskje Van Mensel, Karen Wuyts, Pedro Pinho and Roeland Samson worked on the conception and
606 design of the study. Anskje Van Mensel, Pedro Pinho, Babette Muyshondt and Marta Alos Orti
607 substantially contributed to the acquisition of the data. Anskje Van Mensel and Karen Wuyts worked
608 on the analysis and interpretation of the data. The first draft of the manuscript was written by Anskje
609 Van Mensel. Karen Wuyts, Pedro Pinho, Babette Muyshondt, Cristiana Aleixo, Marta Alos Orti, Joan
610 Casanelles-Abella, François Chiron, Tiit Hallikma, Lari Laanisto, Marco Moretti, Ülo Niinemets, Piotr
611 Tryjanowski and Roeland Samson commented on previous versions of the manuscript. All authors read
612 and approved the final manuscript.

613 *Ethical Approval*

614 Not applicable

615 *Consent to participate*

616 Not applicable

617 *Consent to publish*

618 Not applicable

619 *Availability of data and materials*

620 Not applicable

621

622 **References**

623 Baldacchini C, Castanheiro A, Maghakyan N et al (2017) How does the amount and composition of PM
624 deposited on *Platanus acerifolia* leaves change across different cities in Europe? Environ Sci
625 Technol 51:1147-1156. <https://doi.org/10.1021/acs.est.6b04052>

626 Brignole D, Drava G, Minganti V et al (2018) Chemical and magnetic analyses on tree bark as an
627 effective tool for biomonitoring: A case study in Lisbon (Portugal). *Chemosphere* 195:508–514.
628 <https://doi.org/10.1016/j.chemosphere.2017.12.107>

629 Castanheiro A, Samson R, De Wael K (2016) Magnetic- and particle-based techniques to investigate
630 metal deposition on urban green. *Sci Total Environ* 571:594–602.
631 <https://doi.org/10.1016/j.scitotenv.2016.07.026>

632 Castanheiro A, Wuyts K, Hofman J et al (2021) Morphological and elemental characterization of leaf-
633 deposited particulate matter from different source types: a microscopic investigation. *Environ*
634 *Sci Pollut Res* 28:25716–25732. <https://doi.org/10.1007/s11356-021-12369-z>

635 Catinon M, Ayrault S, Clocchiatti R et al (2009) The anthropogenic atmospheric elements fraction: A
636 new interpretation of elemental deposits on tree barks. *Atmos Environ* 43:1124–1130.
637 <https://doi.org/10.1016/j.atmosenv.2008.11.004>

638 Chaparro M, Chaparro M, Castañeda-Miranda A et al (2020) Fine air particles trapped by street tree
639 barks: in situ magnetic biomonitoring. *Environ Pollut* 266:115299.
640 <https://doi.org/10.1016/j.envpol.2020.115229>

641 Climate Change Knowledge Portal (2021) Climatology.
642 <https://climateknowledgeportal.worldbank.org/country/poland/climate-data-historical>.
643 Accessed 21 Nov 2021

644 Copernicus Land Monitoring Service (2012) Urban Atlas 2012. <http://land.copernicus.eu/>. Accessed 1
645 Dec 2018

646 Declercq Y, Samson R, Van De Vijver E et al (2020) A multi-proxy magnetic approach for monitoring
647 large-scale airborne pollution impact. *Sci Total Environ* 743:140718.
648 <https://doi.org/10.1016/j.scitotenv.2020.140718>

649 Drava G, Ailuno G, Minganti V (2020) Trace Element Concentrations Measured in A Biomonitor (Tree
650 Bark) for Assessing Mortality and Morbidity of Urban Population: A New Promising Approach for
651 Exploiting the Potential of Public Health Data. *Atmosphere* 11. doi:10.3390/atmos11080783

652 Estonian Weather Service (2021) Annual precipitation. [https://www.ilmateenistus.ee/kliima/climate-](https://www.ilmateenistus.ee/kliima/climate-maps/precipitation/annual/?lang=en)
653 [maps/precipitation/annual/?lang=en](https://www.ilmateenistus.ee/kliima/climate-maps/precipitation/annual/?lang=en). Accessed 11 Dec 2021

654 European Environment Agency (EEA) (2020) Air quality in Europe - 2020 report

655 European Environment Agency (EEA) (2021) European city air quality viewer.
656 <https://www.eea.europa.eu/themes/air/urban-air-quality/european-city-air-quality-viewer>.
657 Accessed 11 Dec 2021

658 Eurostat (2021) Population density by NUTS 3 region.
659 [https://appsso.eurostat.ec.europa.eu/nui/show.do?query=BOOKMARK_DS-115323_QID_-](https://appsso.eurostat.ec.europa.eu/nui/show.do?query=BOOKMARK_DS-115323_QID_-5438C657_UID_-)
660 [5438C657_UID_-](https://appsso.eurostat.ec.europa.eu/nui/show.do?query=BOOKMARK_DS-115323_QID_-5438C657_UID_-)

661 3F171EB0&layout=TIME,C,X,0;GEO,B,Y,0;UNIT,B,Z,0;INDICATORS,C,Z,1;&zSelection=DS-
 662 115323UNIT,PER_KM2;DS-115323INDICATORS,OBS_FLAG;&rankName1=UNIT_1_2_-
 663 1_2&rankName2. Accessed 11 Dec 2021

664 Fowler D, Pilegaard K, Sutton MA et al (2009) Atmospheric composition change: ecosystems-
 665 atmosphere interactions. *Atmos Environ* 43:5193–5267.
 666 <https://doi.org/10.1016/j.atmosenv.2009.07.068>

667 Hansard R, Maher BA, Kinnersley R (2011) Biomagnetic monitoring of industry-derived particulate
 668 pollution. *Environ Pollut* 159:1673–1681. <https://doi.org/10.1016/j.envpol.2011.02.039>

669 Hofman J, Wuyts K, Van Wittenberghe S et al (2014a) On the link between biomagnetic monitoring and
 670 leaf-deposited dust load of urban trees: Relationships and spatial variability of different particle
 671 size fractions. *Environ Pollut* 192:285–294. <https://doi.org/10.1016/j.envpol.2014.05.006>

672 Hofman J, Lefebvre W, Janssen S et al (2014b) Increasing the spatial resolution of air quality
 673 assessments in urban areas: A comparison of biomagnetic monitoring and urban scale
 674 modelling. *Atmos Environ* 92:130–140. <https://doi.org/10.1016/j.atmosenv.2014.04.013>

675 Hofman J, Maher BA, Muxworthy AR et al (2017) Biomagnetic Monitoring of Atmospheric Pollution: A
 676 Review of Magnetic Signatures from Biological Sensors. *Environ Sci Technol* 51:6648–6664.
 677 <https://doi.org/10.1021/acs.est.7b00832>

678 Hofman J, Castanheiro A, Nuyts G et al (2020) Impact of urban street canyon architecture on local
 679 atmospheric pollutant levels and magneto-chemical PM₁₀ composition: an experimental study
 680 in Antwerp, Belgium. *Sci Total Environ* 712:135534.
 681 <https://doi.org/10.1016/j.scitotenv.2019.135534>

682 IPMA (2021) List of surface weather stations - long series.
 683 <https://www.ipma.pt/en/oclima/series.longas/list.jsp>. Accessed 11 Dec 2021

684 IRCELINE (2019) ATMO-Street model

685 IRCELINE (2018) ATMO-Street model

686 Kardel F, Wuyts K, Maher BA et al (2011) Leaf saturation isothermal remanent magnetization (SIRM)
 687 as a proxy for particulate matter monitoring: Inter-species differences and in-season variation.
 688 *Atmos Environ* 45:5164–5171. <https://doi.org/10.1016/j.atmosenv.2011.06.025>

689 Kardel F, Wuyts K, Maher BA, Samson R (2012) Intra-urban spatial variation of magnetic particles:
 690 Monitoring via leaf saturation isothermal remanent magnetisation (SIRM). *Atmos Environ*
 691 55:111–120. <https://doi.org/10.1016/j.atmosenv.2012.03.025>

692 Kletetschka G, Žila V, Wasilewski PJ (2003) Magnetic anomalies on the tree trunks. *Stud Geophys Geod*
 693 47:371–379. <https://doi.org/10.1023/A:1023779826177>

694 KMI (2021) Climate statistics of the Belgian municipalities. Antwerp (NIS11002).
695 https://www.meteo.be/resources/climatology/climateCity/pdf/climate_INS11002_9120_nl.pdf.
696 Accessed 11 Dec 2021 (in Dutch)

697 Kottek M, Grieser J, Beck C et al (2006) World map of the Köppen-Geiger climate classification updated.
698 *Meteorol Zeitschrift* 15:259–263. <https://doi.org/10.1127/0941-2948/2006/0130>

699 Lefebvre W, Degrawe B, Beckx C et al (2013) Presentation and evaluation of an integrated model chain
700 to respond to traffic- and health-related policy questions. *Environ Model Softw* 40:160–170.
701 <https://doi.org/10.1016/j.envsoft.2012.09.003>

702 Matzka J, Maher BA (1999) Magnetic biomonitoring of roadside tree leaves: Identification of spatial
703 and temporal variations in vehicle-derived particulates. *Atmos Environ* 33:4565–4569.
704 [https://doi.org/10.1016/S1352-2310\(99\)00229-0](https://doi.org/10.1016/S1352-2310(99)00229-0)

705 Météo-France (2021) Climate Paris-Montsouris - normals.
706 <https://meteofrance.com/climat/normales/france/ile-de-france/paris-montsouris>. Accessed 11
707 Dec 2021 (in French)

708 Meteoblue (2021) Weather History & Climate.
709 <https://www.meteoblue.com/en/weather/historyclimate/climatemodelled/>. Accessed 11 Dec
710 2021

711 MeteoSwiss (2021) Climate normals. Norm value charts.
712 [https://www.meteoswiss.admin.ch/home/climate/swiss-climate-in-detail/climate-](https://www.meteoswiss.admin.ch/home/climate/swiss-climate-in-detail/climate-normals/norm-value-charts.html?filters=precip_9120_yy)
713 [normals/norm-value-charts.html?filters=precip_9120_yy](https://www.meteoswiss.admin.ch/home/climate/swiss-climate-in-detail/climate-normals/norm-value-charts.html?filters=precip_9120_yy). Accessed 11 Dec 2021

714 Mitchell R, Maher BA (2009) Evaluation and application of biomagnetic monitoring of traffic-derived
715 particulate pollution. *Atmos Environ* 43:2095–2103.
716 <https://doi.org/10.1016/j.atmosenv.2009.01.042>

717 Moreira TCL, de Oliveira RC, Amato LFL et al (2016) Intra-urban biomonitoring: Source apportionment
718 using tree barks to identify air pollution sources. *Environ Int* 91:271–275.
719 <https://doi.org/10.1016/j.envint.2016.03.005>

720 Moreno E, Sagnotti L, Dinarès-Turell J et al (2003) Biomonitoring of traffic air pollution in Rome using
721 magnetic properties of tree leaves. *Atmos Environ* 37:2967–2977.
722 [https://doi.org/10.1016/S1352-2310\(03\)00244-9](https://doi.org/10.1016/S1352-2310(03)00244-9)

723 Muhammad S, Wuyts K, Samson R (2020) Immobilized atmospheric particulate matter on leaves of 96
724 urban plant species. *Environ Sci Pollut Res* 27:36920–36938. [https://doi.org/10.1007/s11356-](https://doi.org/10.1007/s11356-020-09246-6)
725 [020-09246-6](https://doi.org/10.1007/s11356-020-09246-6)

726 Pinheiro J, Bates D, DebRoy S, Sarkar D RCT (2021) nlme: Linear and Nonlinear Mixed Effects Models

727 Pöschl U (2005) Atmospheric aerosols: Composition, transformation, climate and health effects.
728 *Angew Chemie - Int Ed* 44:7520–7540. <https://doi.org/10.1002/anie.200501122>

729 QGIS Development Team (2020) QGIS Geographic Information System. Open Source Geospatial
730 Foundation Project.

731 R Core Team (2021) R: A language and environment for statistical computing.

732 Revuelta MA, McIntosh G, Pey J et al (2014) Partitioning of magnetic particles in PM10, PM2.5 and
733 PM1 aerosols in the urban atmosphere of Barcelona (Spain). *Environ Pollut* 188:109-117.
734 <http://dx.doi.org/10.1016/j.envpol.2014.01.025>

735 Sawidis T, Breuste J, Mitrovic M et al (2011) Trees as bioindicator of heavy metal pollution in three
736 European cities. *Environ Pollut* 159:3560–3570. <https://doi.org/10.1016/j.envpol.2011.08.008>

737 Villarroya-Villalba L, Casanelles-Abella J, Moretti M et al (2021) Response of bats and nocturnal insects
738 to urban green areas in Europe. *Basic Appl Ecol* 51:59–70.
739 <https://doi.org/10.1016/j.baae.2021.01.006>

740 Wegiel A, Malinski T, Bocianowski J et al (2017) Equations for predicting age of black locust (*Robinia*
741 *pseudoacacia* L.) based on the tree circumference. *Sylvan* 161:831–841 (in Polish)

742 WHO (2018) Health, environment and climate change: report by the Director-General. *World Heal*
743 *Organ* 2016:1–7

744 Wickham H (2016) *ggplot2: Elegant Graphics for Data Analysis*. Springer-Verlag New York

745 Wuyts K, Hofman J, Wittenberghe S Van et al (2018) A new opportunity for biomagnetic monitoring of
746 particulate pollution in an urban environment using tree branches. *Atmos Environ* 190:177–187.
747 <https://doi.org/10.1016/j.atmosenv.2018.07.014>

748 Zhang C, Huang B, Piper JDA, Luo R (2008) Biomonitoring of atmospheric particulate matter using
749 magnetic properties of *Salix matsudana* tree ring cores. *Sci Total Environ* 393:177–190.
750 <https://doi.org/10.1016/j.scitotenv.2007.12.032>